Available online at www.sciencedirect.com
SCIENCE DIRECT
ELSEVIER
Coordination Chemistry Reviews 250 (2006) 1710–1723
COORDINATION CHEMISTRY REVIEWS
www.elsevier.com/locate/ccr

Review

Porphyrin-containing molecular squares: Design and applications

Suk Joong Lee, Joseph T. Hupp *

Department of Chemistry, Northwestern University, 2145 Sheridan Road, Evanston, IL 60208, United States

Received 17 September 2005; accepted 12 January 2006
Available online 3 March 2006

Contents

Abstract

Coordinative directed assembly has been used by a number of research groups to obtain molecular squares featuring porphyrin components. The syntheses and functional behavior of these compounds are reviewed.

Keywords: Molecular square; Porphyrin; Supramolecular; Catalysis; Sensing

1. Introduction

Porphyrins hold a special place in modern chemistry. Porphyrins and porphyrin-like compounds are ubiquitous in Nature, functioning as catalysts, light collectors, energy movers, and small-molecule binders and transporters. While these molecules sometimes exist as isolated entities, often they appear as well-defined assemblies—for example, as light harvesting complexes in photosynthetic machinery [1]. These ensembles have no doubt provided inspiration for designing and using artificial assemblies of porphyrins. Among the many interesting concepts, "devices", and applications demonstrated are photo-driven molecular switches [2], artificial photosynthetic systems [3], fluorescence-based chemical sensors [4], photonic wires [5], template-directed synthesis [6], reaction catalysis [7], and anti-cancer pharmaceutical behavior [8]. Among the many demonstrated organizational motifs are linear chains [8,9], cyclic oligomers [10], squares, dendrimers [11], sheets and tapes [12], stars [13], and rosettes [14]. The detailed organizational features of these motifs are important because functional behavior often depends on achieving or avoiding π–π stacking, fixing conformations, and attaining optimal orientations and spacings.

* Corresponding author. Tel.: +1 8474913504; fax: +1 8474917713.
E-mail address: j-hupp@northwestern.edu (J.T. Hupp).

0010-8545/$ – see front matter © 2006 Elsevier B.V. All rights reserved.
doi:10.1016/j.ccr.2006.01.015

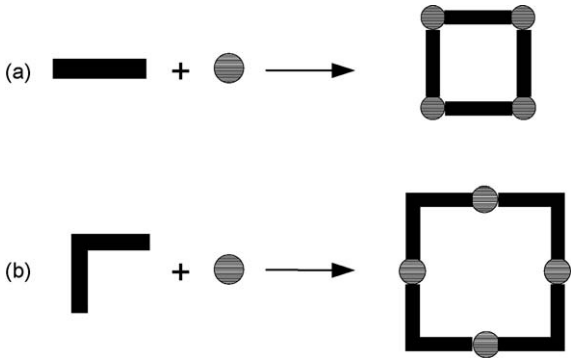

Scheme 1.

Here we review syntheses and applications involving one specific motif: the molecular square, and one synthetic strategy: coordination-based directed assembly. The motif has proven to be a versatile one, facilitating demonstrations of molecular recognition, catalysis, light harvesting, and molecular sieving. The synthetic strategy has proven to be a remarkably efficient and effective one.

Beyond the scope of our discussion are interesting coordinatively linked *dimeric* assemblies such as **1**, that can be viewed as defining square-like cavities [15]. Also beyond the scope are tetra-porphyrinic squares assembled using carbon rather than coordination chemistry [16,17].

2. Synthesis of porphyrin squares

Porphyrin molecular squares are good examples of the application of the principles of coordination-based directed assembly. This approach often offers advantages over classical covalent-bonding-based carbon chemistry [18]. One of these is easy access to ∼90° bond angles. The directed assembly approach takes advantage of square planar and octahedral transition metal coordination to bind multi-functional ligands in linear (180°) or right angle orientations with respect to each other (Scheme 1). For porphyrin squares, the ligands are di-functional and can correspond either to corner units (e.g. 5,10-derivatized porphyrins) or edges (e.g. 5,15-derivatized porphyrins).

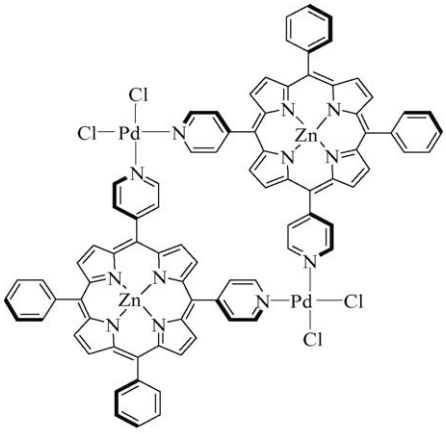

1

Another advantage has to do with what Sugiura has called "the battle for yield" [19]. Cyclic porphyrin oligomer formation via covalent bonding tends to be a low yield process, even when tricks like high dilution and templating are used. The problem is the irreversibility of carbon–carbon bond formation under most conditions, resulting in the formation of a range of kinetic products.

In contrast, directed assembly tends to give high yields, at least if careful attention is given to reaction conditions and solvent. The high yields are a consequence of forming mainly thermodynamic products—which, in turn, is a consequence of the kinetic lability (at least under reaction conditions) of the metal–ligand bonds used. The ability to *un*make bonds and reform new ones until a low-energy structure is obtained is often facilitated by using weakly coordinating solvents. By acting as temporary ligands, these help to maintain the solubility of various fragments and open-chain oligomers, yet are displaceable for cycle formation.

Cyclic structures are enthalpically favored over open ones because a larger number of metal–ligand bonds can be formed. Right-angle containing cycles are enthalpically favored over other cycles because strain is minimized. Finally, small cycles are favored over larger ones for entropic reasons. Consequently, square assemblies often represent lowest energy structures, although with semi-flexible ligands – less subject to strain – triangular assemblies are occasionally favored [20].

2.1. Assembly of porphyrin squares with Pd and Pt

A report by Drain and Lehn in 1994 was the first to describe the coordinative assembly of a porphyrin square [21]. As shown in Scheme 2, the formation of the neutral tetranuclear cyclic assembly **4** was achieved by simple mixing of 5,10-(4-pyridyl)-15,20-phenyl-porphyrin (*cis*-DPyDPP, **2a**) or its Zn complex **2b** with one equivalent of *trans*-$Pd(NCPh)_2Cl_2$, at micromolar concentrations. The estimated size of the squares, as defined by the metal corners is roughly 20 Å × 20 Å. Combining *cis*-$Pd(NCPh)_2Cl_2$, in a similar manner, with micromolar solutions of **2a** or **2b** produced cyclic dimers in high isolated yield, rather than tetramers. Products were characterized by NMR spectroscopy and mass spectrometry combined with UV–vis spectrophotometry and vapor-phase osmometry. A fluorescence polarization study provided additional support for square formation.

UV–vis titrations of porphyrin solutions of **2** with either *trans*- or *cis*-$Pd(NCPh)_2Cl_2$ showed clear isosbestic points. The titrations indicate that dimeric or tetrameric cycle formation occurs rapidly. They also indicate that cycle formation is an all-or-nothing process thermodynamically; observable amounts of partially formed cycles are absent. The primary visible-region porphyrin monomer absorption band (Soret band) is red shifted by 6–8 nm and significantly broadened upon square formation. At the same time, the fluorescence quantum yields for **2a** and **2b** decrease by more than two-fold, evidently largely because of heavy atom (Pd) acceleration of singlet-to-triplet excited-state intersystem crossing.

Porphyrin-containing ligands are particularly interesting because they can serve as either linear or angular components –

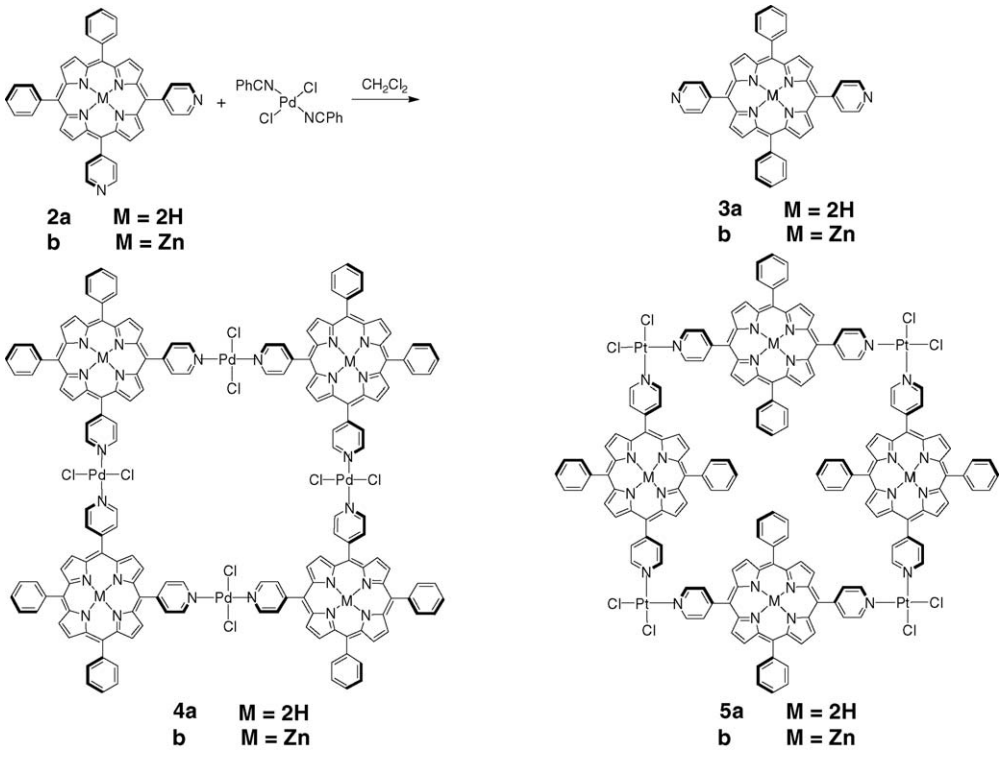

Scheme 2.

edges or corners – depending on the location of donor functional groups. In the same paper where square **4a** and **4b** were reported, Drain and Lehn described the synthesis of the neutral squares **5a** and **5b** from *cis*-Pt(NCPh)$_2$Cl$_2$ and the 5,15-derivatized isomers of **2a** and **2b** [21]. Compared with palladium(II), square formation with platinum(II) requires harsher conditions (refluxing toluene) but yields more robust assemblies.

Milic et al. have noted that in compounds like **4** the porphyrins lie in a common plane, so would be expected to form columnar stacks under the right conditions [22]. Compounds like **5**, on the other hand, are not necessarily arranged in the same way. Milic et al. argue, on the basis of molecular mechanics calculations, that a hypothetical analogue of **5**, lacking phenyl substituents, would prefer a geometry in solution in which two porphyrins are oriented cofacially and normal to the plane defined by the four platinum atoms. The other two are highly tilted and nearly coplanar. The porphyrin edges or walls of a derivative of **4** featuring dodecyloxy tails on the eight phenyls are thought to be arranged in a roughly square pyramidyl fashion. A similar geometry has been inferred for an octa-cationic square (discussed below) on the basis of ^{1}H and ^{31}P NMR measurements [23]. Atomic force microscopy (AFM) measurements of deposits of the dodecyloxyphenyl functionalized square on glass are consistent with a box-like geometry (all four porphyrins perpendicular to the tetra-metallic plane) where the boxes lie on their sides.

In addition to neutral squares, Drain and Lehn alluded to the formation of charged squares based on replacement of chloride ligands with ethylenediamine [21]. However, no further information was offered. Stang and co-workers showed that squares with overall +8 charges could be assembled by using diphosphines to enforce a cis geometry at sites initially occupied by labile trifluoromethane sulfonate (triflate, OTf$^-$) ligands [23,24]. Two examples based on Pd(II) corners are shown in Scheme 3. These researchers also prepared Pt(II) analogues as well as several featuring porphyrin ligands **7a** or **7b** in place of **6a** or **6b**. Like the squares reported by Drain and Lehn, these assemblies are weakly fluorescent in solution at ambient temperature. Yields for isolated products ranged from 78% to 94%, underscoring the efficiency of well-designed directed assembly schemes. Evidence for square formation came chiefly from ^{1}H and ^{31}P NMR measurements, although in some cases mass spectral evidence was also obtained.

By using chiral binapthol-functionalized diphosphines as ligands for palladium(II), Stang et al. were able to prepare chiral porphyrin squares [24]. Evidence for chirality was provided by induced circular dichroism in the porphyrin absorption spectra. In addition to defining chirality and coordination geometry, phosphine and diphosphine ligands are useful for eliciting solubility [23,25].

Scheme 4 shows an interesting example of the formation of a charged square featuring porphyrins as corners rather than edges [23]. Evidence for cycle formation again came chiefly from NMR measurements. For example, since the pyridyl-containing porphyrin ligands have characteristic α-pyridyl protons in the ^{1}H NMR spectra, these proton signals were expected (and found) to disappear when the correct corner/connector stoichiometry was reached, with a new set of signals appearing up-field.

Finally, Drain and co-workers have reported the formation of a square of squares, **11**, using *trans*-Pd(NCPh)$_2$Cl$_2$ and a 1:4:4 ratio of tetrapyridyl (X-shaped), tripyridyl (T-shaped),

and dipyridyl (L-shaped) porphyrins [26]. Formation occurs in less than 30 min at room temperature and in ∼90% yield (solution phase, 2 μM total concentration). Obviously, at such low concentration the evidence for formation of the nonamer is indirect. At 10 μM total porphyrin concentration, ^{1}H NMR measurements indicated a nonamer yield of around 70%. The most compelling evidence for formation of the desired nine-porphyrin array is its appearance in an electrospray mass spectrum. The planar arrays appear to stack in columns when exposed to glass surfaces, as evidenced by AFM measurements. On gold surfaces, arrays are present as isolated assemblies and as stacks of two or three assemblies, as evidenced by scanning tunneling microscopy measurements [27,28].

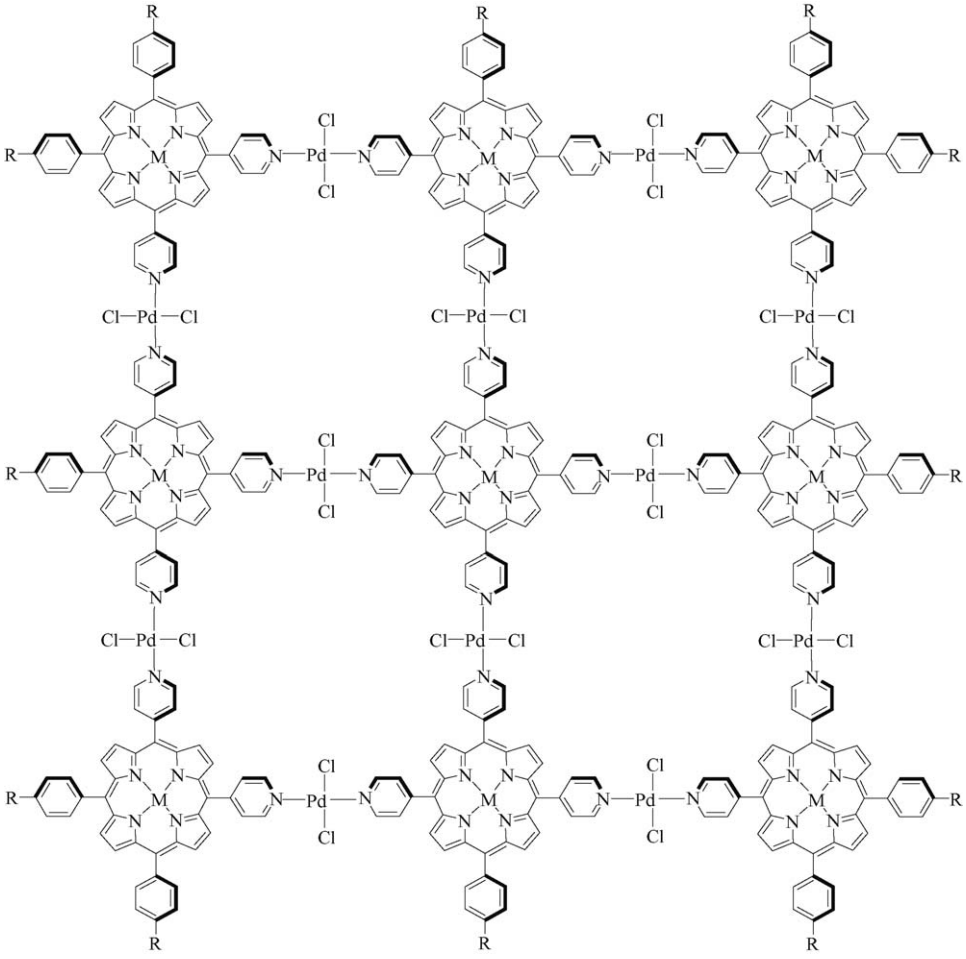

11 a = 2H **R = CH_3, $C(CH_3)_3$**
b = Zn

2.2. Assembly of squares with rhenium as corners

The formation of squares featuring *fac*-Re(CO)$_3$Cl corners has been described by Slone and Hupp (Scheme 5) [29]. The strong trans labilizing effect of CO serves to activate two (and only two) carbonyls for substitution—presumably first by solvent molecules (tetrahydrofuran, THF) and then by pyridyl porphyrins. As with other metal-linked porphyrin squares, yields for rhenium based squares are high. Reactions can take up to 2 days to complete under refluxing conditions, but the resulting assemblies are stable even when dissolved in solvents qualifying as good ligands. A potentially important difference between these assemblies and the previously described platinum and palladium containing assemblies is the octahedral coordination of the metal center. In principle, this could open up routes to more complex structures in which functional ligands, oriented perpendicular to the plane of the square, replace chloride ligands. To our knowledge, however, this idea has not yet been demonstrated.

Scheme 5 shows a single isomer with respect to chloro ligand orientation—in this case, alternating up/down orientations. In principle, three others should exist (all up, three up and one down, two up followed by two down). While no experimental information is available with regard to isomer formation, it is reasonable to assume that all four are formed, presumably in statistically defined proportions.

Characterization of squares such as **12** has proven challenging because they resist crystallization and in most cases they are not volatilized by the standard techniques employed in mass spectrometry. Infrared spectroscopy in the carbonyl stretching region

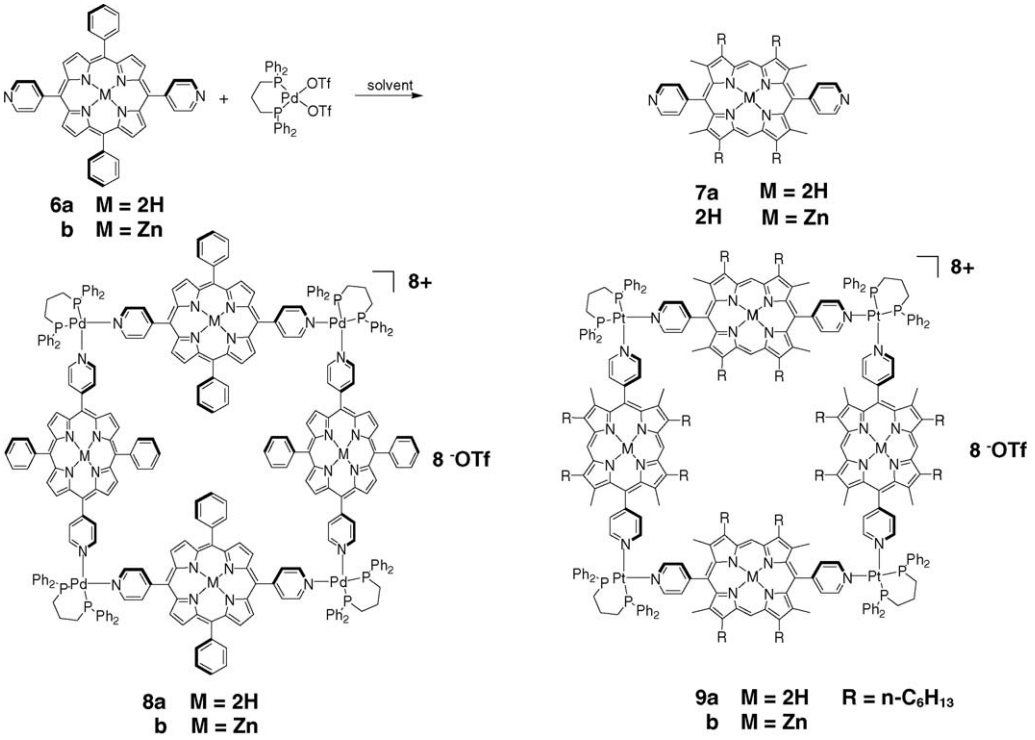

Scheme 3.

is distinctive for *fac*-tricarbonyl rhenium(I) units and ^{1}H NMR is diagnostic of pyridine coordination, but neither establishes square formation with certainty. Approximate molecular weight determination by vapor-phase osmometry has been used in one instance to confirm tetramer formation [30]. Gel permeation chromatography has been proposed for determining sizes of squares and for distinguishing squares from triangles [31], since retention times vary inversely with size. Pulsed-field-gradient NMR, which measures coefficients for self-diffusion, has also been considered [32] since the coefficients vary inversely with assembly size (Fig. 1) [33]. An extremely powerful method, although one not yet widely used in supramolecular coordination chemistry, is synchrotron-based solution-phase X-ray scattering and molecular diffraction [34].

Bélanger et al. explored the idea of tailoring porphyrin walls by axially ligating imines, amines, and azines to the available Zn(II) centers [35]. This is a mechanism for imparting functionality to the square cavity (e.g. sensing, catalysis, etc.), as discussed further below. (In the presence of ligands, Zn(II) is five-coordinate, not six, so binds only one ligand axially.) As one might guess, di-functional ligands capable of spanning the square cavity are bound more strongly than ligands having only one attachment point. The tailoring idea works, despite the affinity of Re(I) for imines and azines, because the rhenium sites are substitution inert at room temperature.

Slone observed that either 5,10,15,20-(4-pyridyl)porphyrin (TPyP) or the dipyridyl porphyrin, **7**, could be bound within the cavity of **12** in noncompetitive (weakly Lewis basic) solvents such as methylene chloride [29]. The association constant for two-point binding of **7** was found to be about three orders of magnitude larger than one-point binding by pyridine itself. Increasing the number of Zn–N interactions to four (TPyP), was found to increase the association constant by only one additional order of magnitude. Evidently, the energetic cost of arranging **12** in a box-like conformation to accommodate ligation of all four zinc ions largely offsets the gains obtained by increasing the number of ligand–metal interactions. A computational study by Ellis and co-workers supports the notion that the lowest energy conformation for the square in the absence of TPyP is not a box-like structure [36].

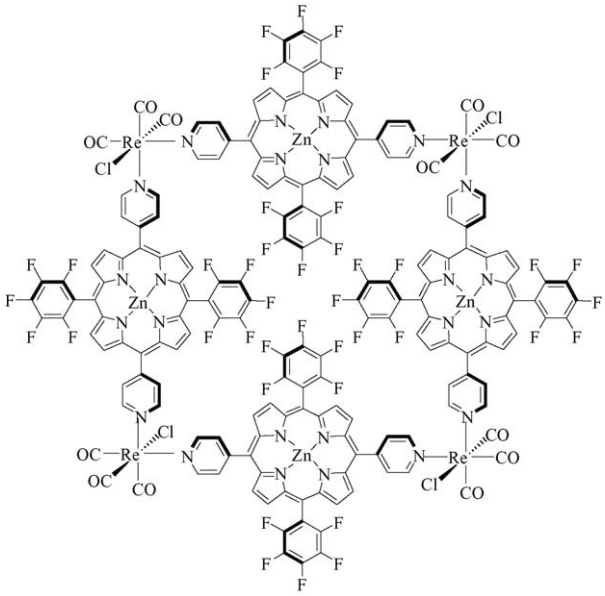

13

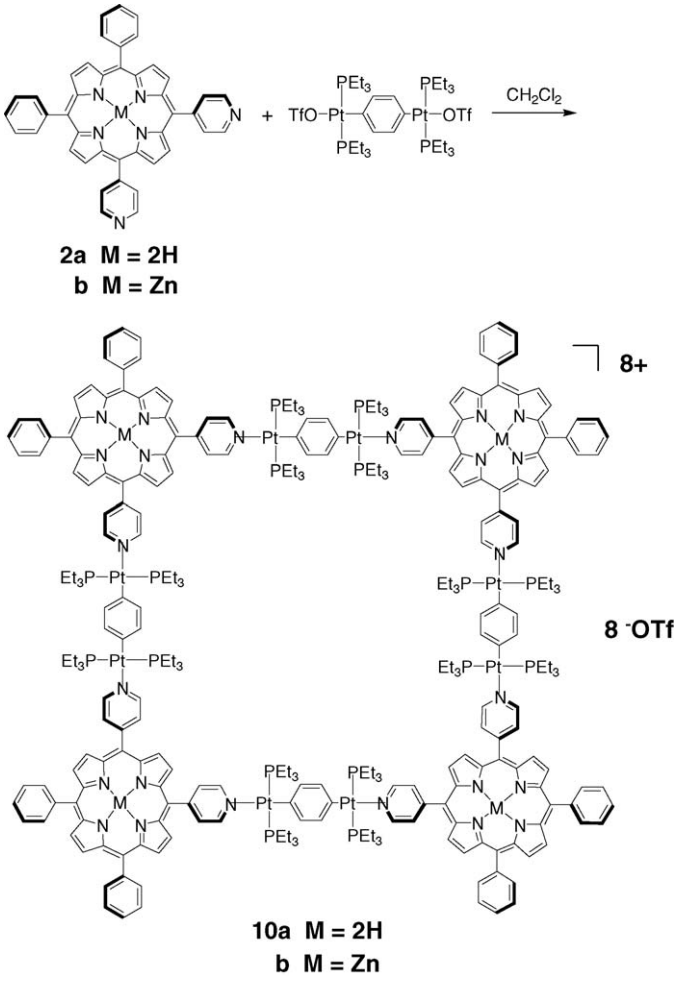

Scheme 4.

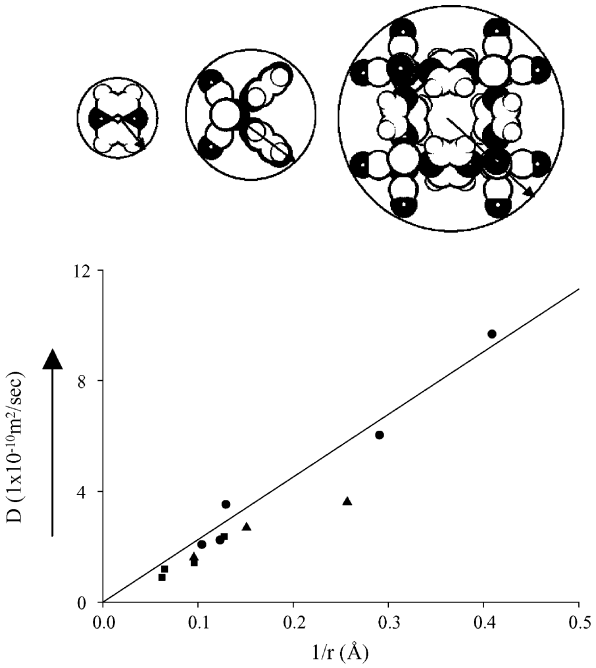

Fig. 1. Top: Approximation of molecular radii for free ligand (pyrazine), rhenium corner, and rhenium square. Bottom: Diffusion coefficient vs. the reciprocal of the estimated radii for various ligand (●), corner (▲), and square (■) species. Figure from Ref. [32].

Molecular square **12** weakly fluoresces in methylene chloride as solvent. The singlet lifetime is reported to be 2.4 ns [29]. The weak luminescence and relatively short lifetime are presumably consequences of accelerated intersystem crossing caused by proximal heavy atoms (rhenium). When bound as a guest, TPyP is reported to quench ∼90% of the luminescence of **12**. The mechanism of quenching was not established.

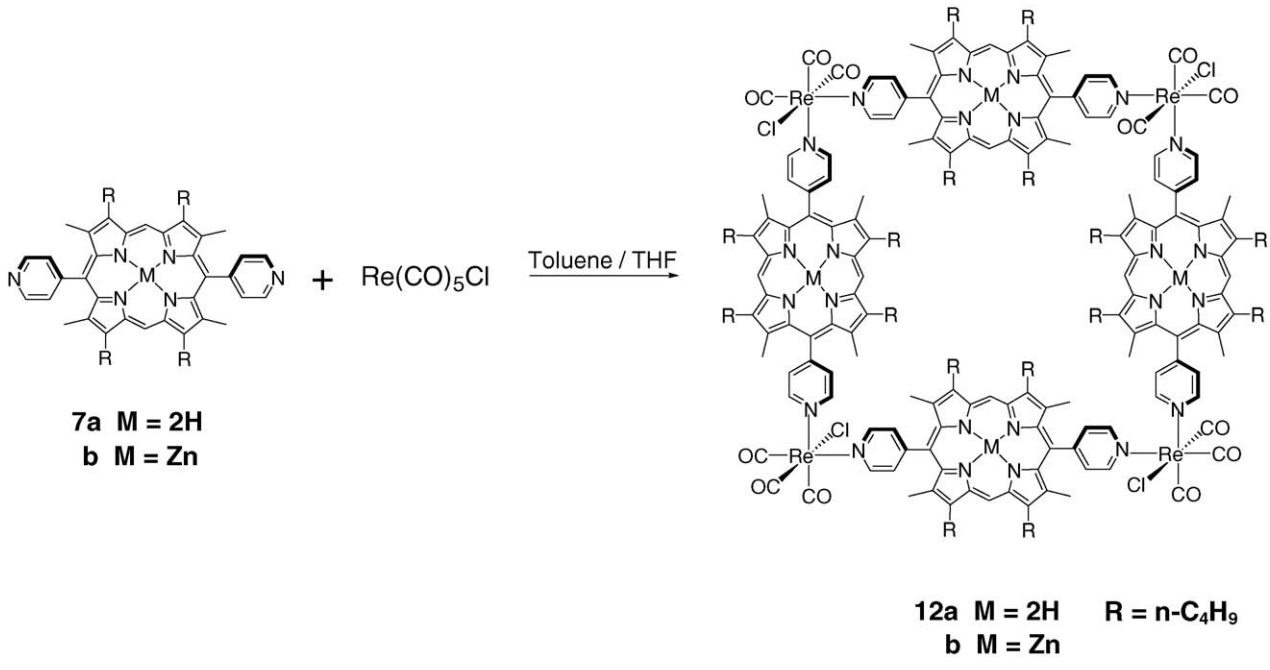

Scheme 5.

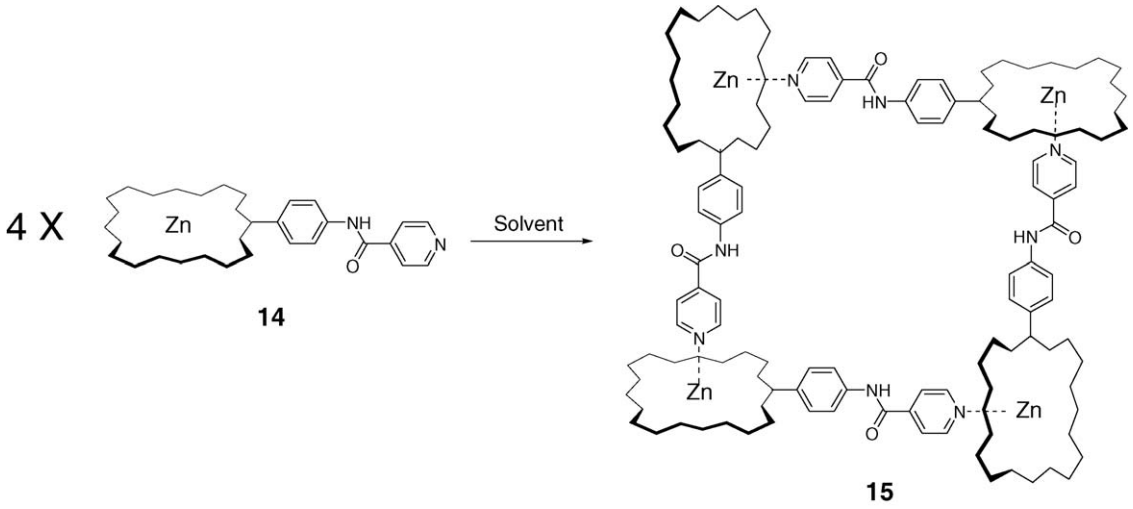

Scheme 6.

Splan was able to increase the binding constant for 4-(phenyl)pyridine from 1.5×10^4 to $1.35 \times 10^5\ M^{-1}$ in methylene chloride as solvent by discarding **12**'s alkyl substitituents and adding perfluorophenyl groups (see assembly **13)** [37]. The perfluorinated substituents are strongly electron withdrawing, so significantly increase the Lewis acidity of the Zn(II) sites and strengthen the Zn–N interaction.

Despite the presence of rhenium, assemblies **12**, **13** and related porphyrin squares are luminescent, although less so than free porphyrin ligands.

2.3. Square formation via axial ligation

Axial coordination of porphyrin-pendant pyridines to zinc(II) porphyrins has been exploited by Chi and co-workers to construct the cyclic tetramer shown in Scheme 6. The assembly reaction lies mainly to the right when the initial reactant concentration is 10^{-4} M, but mainly to the left when it is 10^{-8} M [38]. Square formation is accompanied by a red shift in the Soret band in the UV–vis absorption spectrum and by very large up-field shifts in NMR resonances for the pyridyl protons due to their proximity to the porphyrin ring current. Osuka and co-workers have reported on the formation of closely related assemblies featuring pyridine (only), phenylpyridine, or biphenylpyridine pendant groups [39], with characterization of the pyridine version by single-crystal X-ray diffraction [40].

A distinctive feature of this mode of assembly is an appreciable loss of porphyrin torsional motion. This, together with smaller cavity sizes in comparison to the squares described above, presumably accounts for the formation of diffraction-quality crystals.

Imamura and co-workers have reported on the synthesis of closely related assemblies featuring Ru(II) in place of Zn(II) [41]. One of the objectives was to enhance the stability of the square by strengthening metal/axial-ligand interactions. Ru(II) is six-coordinate in this environment, so possesses a second axial ligand. When the second axial ligand is pyridine, the assembly is stabilized as evidenced by its resistance to dissociation in the presence of excess pyridine. When the second axial ligand is CO, however, the square is readily dissociated by excess pyridine which displaces the pyridyl porphyrin in the Ru(II) coordination sphere. The observation is consistent with the known strong

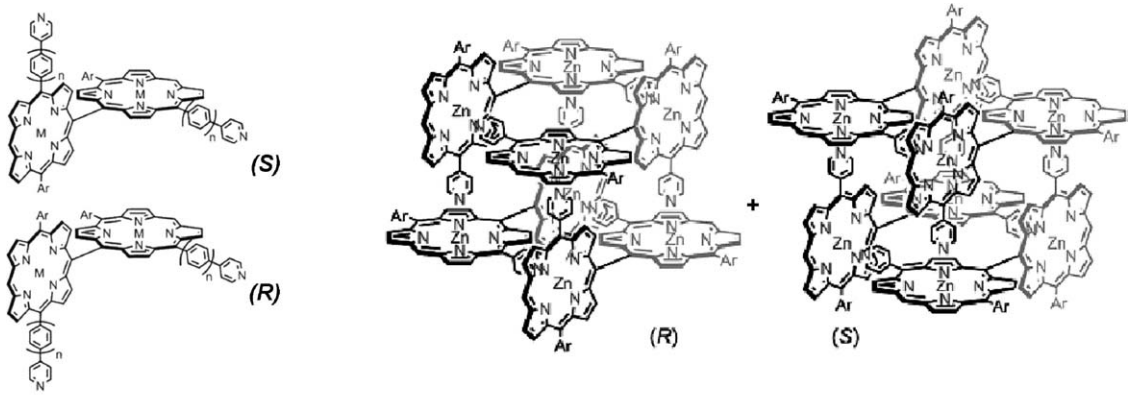

Scheme 7.

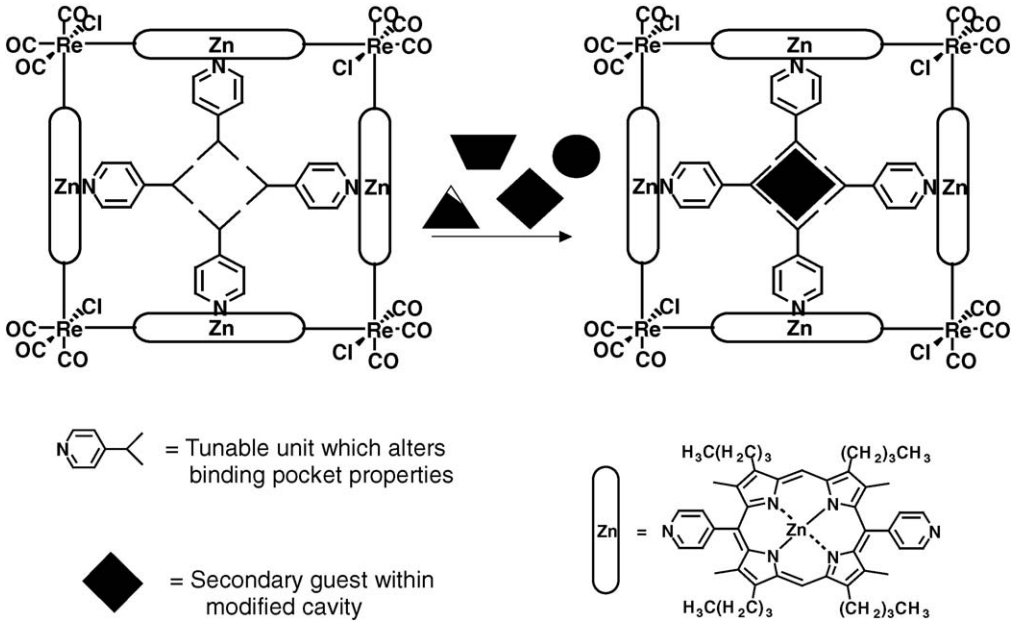

Scheme 8.

trans labilizing effect of CO. Imamura and co-workers have also reported on the synthesis and X-ray structural characterization of rhodium(III) analogues where chloride is the second axial ligand [42]. These are similarly resistant to dissociation.

Osuka and co-workers have elaborated on the axial ligation strategy by using dimeric porphyrins such **16** as building blocks [43]. One might expect these to form a linked pair of square assemblies. This is not the case. In the absence of spacers, the porphyrins comprising the free dimers adopt an orthogonal conformation (Scheme 7) so as to minimize steric interactions between β protons. The geometric orthogonality results in box formation, rather than linked square formation. In principle the boxes can exist in either of two enantiomeric forms. With eight Zn–N interactions per box, the boxes proved stable enough to be resolved by chiral HPLC into mirror image forms.

In collaboration with the Kim group, Osuka and co-workers also examined the photophysical behavior of the assemblies. From time-resolved absorption polarization anisotropy measurements, they were able to estimate the time for Förster type exciton hopping within the photo-excited boxes ($\tau_{hopping} = 48$ ps).

3. Functional porphyrin molecular squares: individual molecules, thin-film aggregates, permeable layer-by-layer assembled structures, and polymeric membranes

3.1. Sensors

The availability of tailorable cavities together with measurable photo-luminescence suggests that porphyrinic squares should be capable of functioning as chemical sensors (Scheme 8). Chang et al. explored this idea in a brief report on sodium and potassium ion sensing by square **12** [44]. A crown ether featuring a pendant pyridine (**18**) was ligated to the square's Zn(II) sites, with concomitant diminution of square luminescence. While the ligand lacks obvious energy- or electron-transfer quenching capabilities, axial ligation of "innocent" species is well known to influence porphyrin fluorescence quantum yields [45]. Upon capture of the cationic analyte the fluorescence intensity was found to increase.

The idea of tailored cavities and chemical sensing was extended to thin films of **12** by Mines et al. [46]. Advantage was taken of both the modest solubility of the square in polar organic solvents and its insolubility in water. The films obtained are amorphous molecular aggregates, with the cavities of individual squares providing both vapor and solution permeability. Micropatterned films were found to be capable of diffracting visible light—for example, the output of a laser pointer. Uptake of guests by films was detected via changes in diffraction efficiency. Nonspecific uptake of volatile organic analytes such as toluene from the vapor phase was examined. Molecular-square cavity functionalization with tris(aminoethyl)amine yielded films that responded specifically to aqueous Zn^{2+}. Functionalization with 1,6-hexanedithiol yielded films responsive to molecular iodine, due to iodine/thiol charge-transfer complex formation.

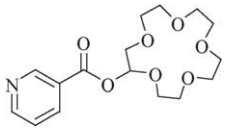

18

3.2. Catalysis

One of the most promising applications of supramolecular coordination chemistry is in catalysis. In principle, cavities could be used to bind reactants selectively, control reaction stereochemistry, or protect highly reactive catalytic sites from

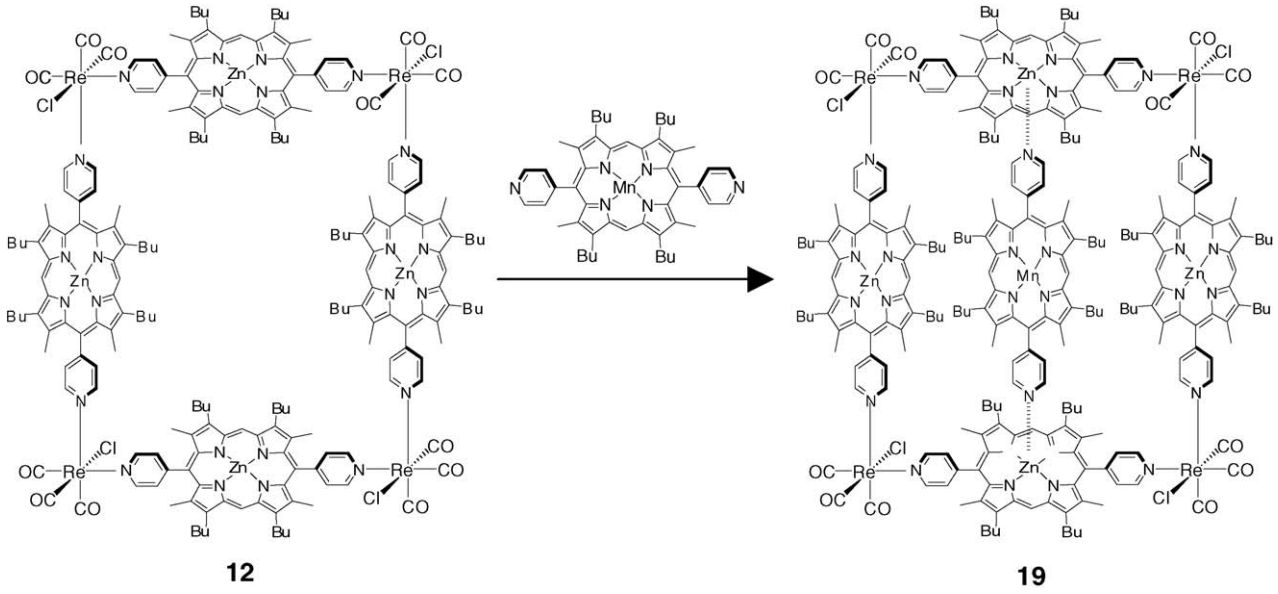

Scheme 9.

interaction with species other than intended substrates. Merlau et al. have reported on the use of square **12** as an encapsulant for manganese porphyrin epoxidation catalysts (Scheme 9) [7]. Manganese porphyrins have been extensively examined previously as epoxidation catalysts [47,48], primarily because of high functional and structural similarity to the iron heme moiety comprising the catalytic center of cytochrome P450. This naturally occurring enzyme is used in the oxidative metabolism of many biological compounds [49]. Unfortunately, the naked manganese porphyrin degrades quickly under catalytic reaction conditions due to the formation of oxo-bridged (Mn–O–Mn) dimers and/or irreversible porphyrin ligand oxidation.

Protective encapsulation of dipyridyl and tetrapyridyl forms of the catalyst within square **12** was found to stabilize the catalysts, extending their lifetimes for olefin epoxidation by an order of magnitude or more—evidently by inhibiting oxo-bridged dimer formation. With the dipyridyl catalyst, the square also induced substrate size selectivity by preventing access to the active site by large substrate molecules. Modifying the molecular-square cavity by ligating pyridine derivatives at two of the Zn(II) sites, while anchoring the catalyst at the other two, resulted in partial tunability of the substrate size selectivity [7]. Limiting the cavity tunability is the torsional flexibility of both the catalyst and the left- and right-hand walls of the assembly shown in Scheme 9. Also limiting the effectiveness of cavity tuning is the possibility of binding the modifier to the square's exterior rather than interior.

3.3. Membranes, films, and molecular sieving

3.3.1. Molecular materials

Noncrystalline molecular-aggregate type films of **12**, obtained simply by solvent evaporation, have proven surprisingly effective as molecular sieves. In one study films were prepared on mesoporous polyester membrane supports that were then used as size-selective barriers to molecular transport between solutions [50]. Transport was observed via UV–vis absorption by the permeant in the receiving solution. Films were found to be permeable to $Fe(bpy)_3^{2+}$ (diameter ~ 13 Å; bpy = 2,2′-bipyridine) and smaller species, but blocking toward Fe(4,7-phenylsulfonate-1,10-phenanthroline)$_3^{4-}$ (diameter ~ 24 Å). No dependence on molecular charge was seen. The findings are consistent with estimated 18 Å diameter for the square cavity. In an additional study the square cavity was partially blocked by binding a fifth dipyridyl porphyrin to two of the four Zn(II) sites (Scheme 9). These cavity-modified films proved permeable to phenol but blocking toward $Fe(bpy)_3^{2+}$.

Fig. 2 illustrates an electrochemical approach to observing molecular sieving. Because the measured current from a redox-active probe can be related directly to molecular flux, electrochemical methods are useful for quantifying transport. Measurements of this kind with films of **12** showed that the flux decreases as the film thickness increases [51,52]. This behavior

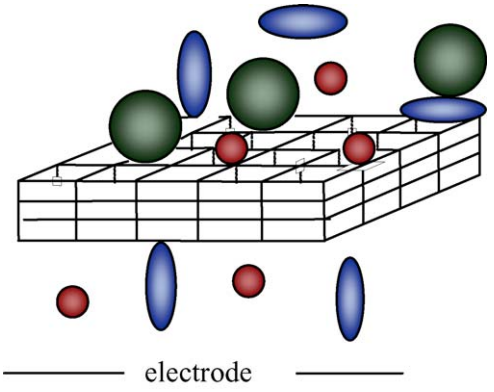

Fig. 2. Schematic representation of film permeation studies using electrochemical technique. For simplicity, film structure is idealized as crystalline rather than disordered.

is indicative of permeation-controlled transport. In other words, transport is limited by diffusion through the film rather than by partitioning from the solution into the film. The absolute magnitude of the flux at a particular thickness was then used to determine the permeability, PD_f, of the probe molecule. (P is the solution-to-film partition coefficient and D_f is the film-based diffusion coefficient.) Measurements of this kind in water as solvent yielded permeabilities that were about 50× smaller than solution-phase diffusion coefficients.

Inclusion of the dipyridyl ligand in the large square cavity yields two rectangular cavities of intermediate size. The resulting modified material is permeable to relatively small species such as $Ru(NH_3)_6^{3+}$ and ferrocene–methanol, but blocking toward a larger probe, $Co(bpy)_3^{2+}$ [52]. Inclusion of TPyP yields four small cavities. This material is readily permeated by iodide (diameter ∼3 Å), but is almost completely blocking toward the larger probe, $Ru(NH_3)_5(4\text{-picoline})^{2+}$. The tunable sieving behavior can be nicely visualized, as shown in Fig. 3, by scanning electrochemical microscopy imaging of film-coated micro-electrodes [51]. Current (molecular flux) is observed only when: (a) the imaging electrode is positioned above the coated microelectrode and (b) the probe molecule can permeate the porphyrin-square film.

3.3.2. *Polymeric materials*

Construction of permeable, microporous polymeric membranes from molecular squares has been also demonstrated [30]. In contrast to molecular-aggregate type materials, the polymeric membranes are swellable, resistant to dissolution in polar organic solvents, and useable without supports. The method used for membrane fabrication was polymerization at the interface of a pair of immiscible liquids. One liquid contained molecular square **21**, functionalized with eight reactive phenol groups, and the other, a bis(acid chloride) linker (Scheme 10).

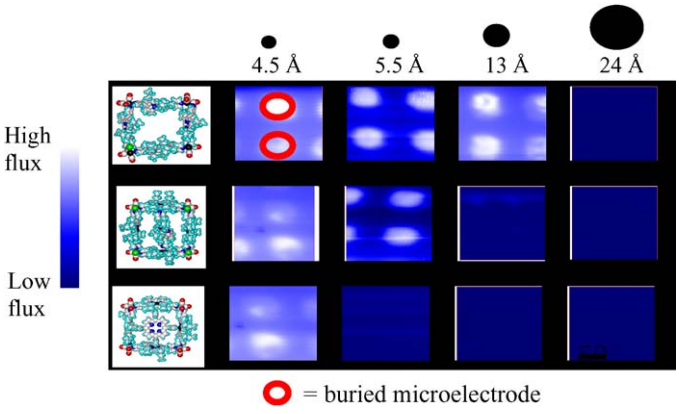

Fig. 3. Scanning electrochemical microscopy images illustrating molecular sieving by molecular-aggregate films. Figure from Ref. [51].

Interfacial polymerization is an attractive approach to membrane fabrication because it is self-limiting and, during the growth phase, membranes are self-healing. Pinhole free membranes ranging in thickness from ∼100 nm to 2.5 μm were prepared. From atomic force microscopy and profilometry measurements, membrane roughness was ca. 10% of thickness. The FT-IR spectra of the polymers show stretches indicative of both the molecular-square subunits and the polyester linkages. The presence of the carbonyl stretches from the $Re(CO)_3Cl$ corners at 2022, 1909, and 1890 cm^{-1}, alkyne stretch from the ethynyl spacer at 2183 cm^{-1}, and secondary amine stretches from the amine linkages at 1648 and 1512 cm^{-1} are evidence of polymer formation based on intact molecular-square subunits.

Membrane permeability with respect to a series of redox-active probe molecules was evaluated using quasi-steady-state cyclic voltammetry, following placement of polymer mem-

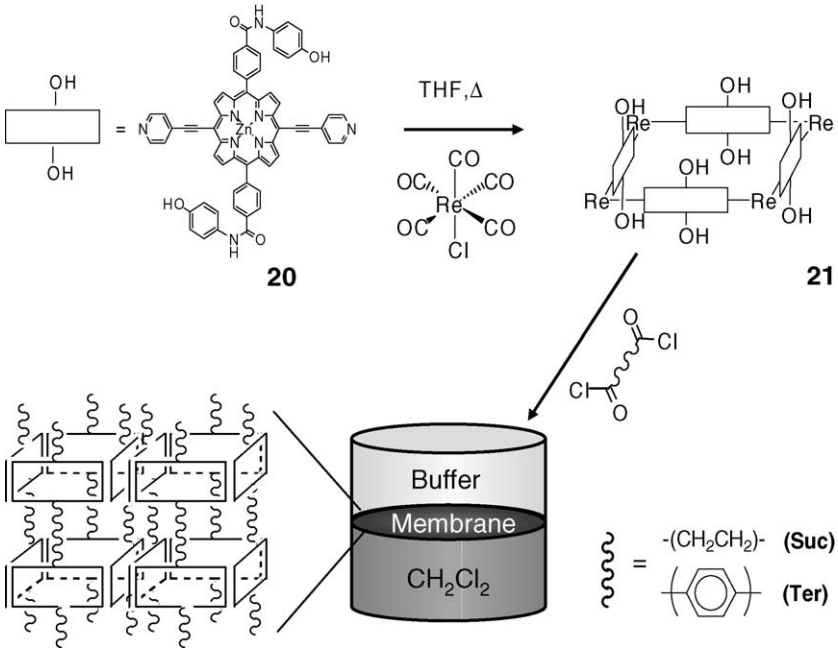

Scheme 10.

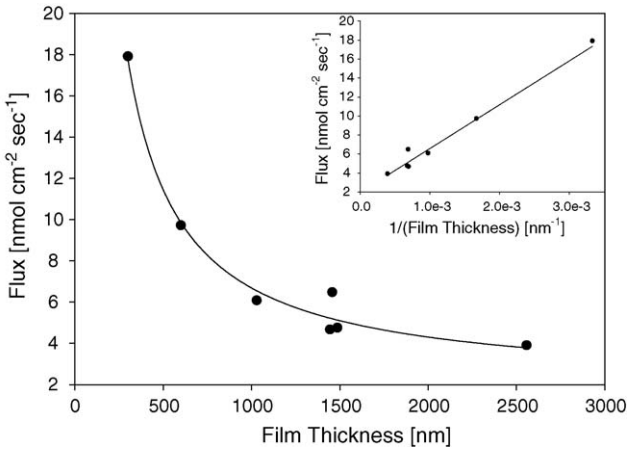

Fig. 4. Probe molecule (FcMeOH, $Fe(CN)_6^{4-}$, $Co(Phen)_3^{2-}$, $Fe(bphen(SO_3)_2)_3^{4-}$, and $Ru(PNI\text{-}phen)_3^{2+}$) flux as a function of polymeric membrane (**21**) thickness. The line is drawn to show a first order inverse fit to the data. Inset shows linearity of the reciprocal plot. Figure from Ref. [30].

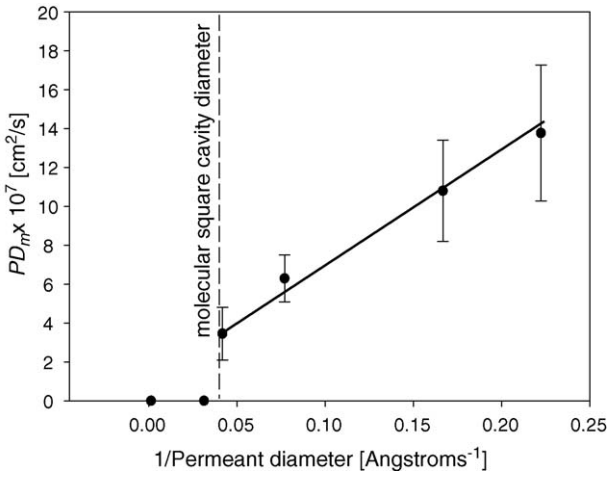

Fig. 5. Dependence of molecular permeability on permeant diameter for transport through polymeric membranes of **21**. Figure from Ref. [30].

branes over platinum microelectrodes. Shown in Fig. 4 is the dependence of molecular flux on polymer film thickness. As mentioned above, the observed inverse correlation is characteristic of permeation-limited, as opposed to partitioning-limited, transport. Permeabilities were found to be more than an order of magnitude larger than measured for molecular-aggregate films.

The polymeric membranes displayed very good condensed-phase molecular sieving behavior, and an unusually sharp permeant size cutoff (Fig. 5). The cutoff correlates well with the size of the molecular-square cavity, suggesting that the cavities define the maximum pore size in the membranes. Additionally, transport studies with a wide range of organic solvents, including THF, pyridine, chloroform, acetonitrile, and acetone,

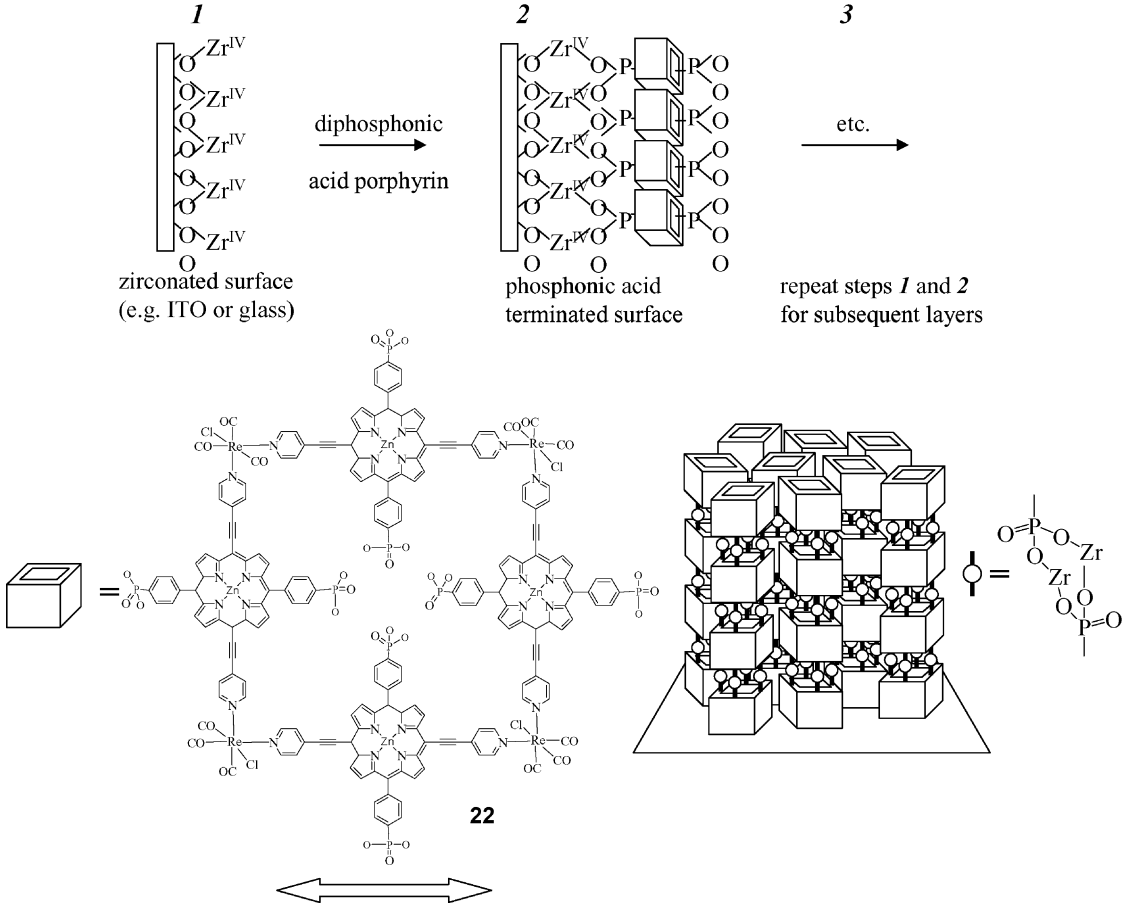

Scheme 11.

demonstrated the advantages in terms of the stability of the membranes over analogous organic-solvent-soluble molecular-aggregate materials.

3.3.3. Layer-by-layer assembled materials

Massari and co-workers have described the fabrication of electrode-supported molecular-square films via a layer-by-layer assembly technique as shown in Scheme 11. Based on chemistry demonstrated previously by Katz et al. [53], Mallouk and co-workers [54], Clearfield [55], and Thompson and co-workers [56], advantage was taken of the strong interaction between Zr(IV) and phosphonates to construct porous films in stepwise fashion. The layer-by-layer assembly method is an attractive one for obtaining pinhole-free films because defects are over-written in subsequent assembly cycles. Typically three cycles were required to obtain molecular-square films that were pinhole-free based on electrochemical measurements.

The approach is also useful for assembling films of precise thickness. For vertical box-like stacking of the squares, a 2.5 nm layer thickness would be expected. Atomic force microscopy measurements of intentionally scratched molecular-square films showed that films increased in thickness by about 1.9 nm per assembly cycle, suggesting that the square's walls are tilted. An X-ray standing wave study using films assembled on Si/Mo X-ray mirrors corroborated the low layer thicknesses and also showed that the amount of zirconium contained in the films is much higher than implied by phosphonate charge compensation [57]. Evidently zirconium dioxide is also formed [58].

Film permeability to redox probes was examined using wall-jet electrochemistry. Molecular sieving behavior was observed, but with a smaller size cutoff than expected based on the cavity diameter for an isolated square. Additionally, the size cutoff was less sharp and PD_f values were much smaller for the layer-by-layer assembled films than for polymer membranes. These differences were ascribed to rigidity for the zirconium phosphonate linked films versus swelling and flexing for the polymeric square material.

3.4. Photoelectrochemical energy conversion

Phosphonated molecular squares have been examined as multilayer sensitizers of indium–tin oxide (conductive glass) surfaces in photoelectrochemical solar cells. Generally these cells convert energy by the following sequence: (a) dyes are photo-excited, (b) energy is transferred from outer layers to the innermost layer of dye molecules, (c) electrons are transferred from the excited inner layer to the transparent electrode, leaving oxidized dye molecules, (d) dyes are restored to their original form by reduction with a redox shuttle, and (e) the oxidized shuttle molecules diffuse to a dark electrode and are reduced, completing the circuit [59]. Multilayer sensitization typically is only marginally better than monolayer sensitization despite the collection of more photons [60]. One of the problems is believed to be difficulty in moving charge-compensating ions within or through chromophoric layers. In principle, this difficulty could be overcome by using porous molecular-square films as light absorbers.

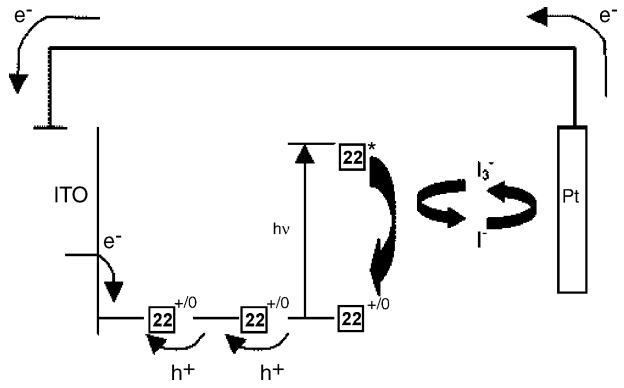

Fig. 6. Mechanism of cathodic current generation by **22**/ITO multilayer electrodes.

A study done in water as solvent with iodide/triiodide as the redox shuttle exhibited the hoped-for systematic increase in photocurrent with increasing number of dye layers [61]. The direction of current flow, however, was the opposite of what was expected. Further study revealed that the cell operated according to the mechanism shown in Fig. 6. The key feature is direct quenching of the photo-excited porphyrinic square by a pre-associated triiodide ion.

4. Conclusions

Coordination-based directed assembly strategies, utilizing mainly Pd(II), Pt(II), Zn(II), and Re(I) chemistry, have been used to prepare several porphyrinic molecular squares. Beginning with the first report in 1994, the approach has generally produced assemblies in high synthetic yield. Post-synthetic tailoring of square cavities has been demonstrated. Organization of squares as porous films or membranes has been demonstrated by layer-by-layer assembly chemistry, liquid/liquid interfacial polymerization, and simple molecular aggregation. Surface stacking of flat squares has also been observed. Proof-of-concept demonstrations of catalysis, chemical sensing, molecular sieving, and photocurrent production have been reported, where the functional behavior is a consequence of the formation of nanometer-scale cavities. In our opinion, the next advances in this area are likely to come from work focused on: (a) spontaneous assembly of higher order structures having less malleable and better defined cavities and displaying more sophisticated guest-recognition behavior, (b) application of new structural characterization methods, especially in solution environments and in thin films, and (c) more sophisticated and useful demonstrations of functional behavior. Catalysis, in particular, may be an area where "hollow molecules" such as porphyrinic squares and related assemblies can be used to real advantage.

Acknowledgments

We gratefully acknowledge the U.S. Department of Energy, Basic Energy Sciences Offices, for support of our own work on photophysics and energy conversion (Grant No. DE-FG87ER13808) and on membranes and molecular sieving (Grant No. DE-FG02-01ER15244), and the Northwestern Insti-

tute for Environmental Catalysis for support of our work on catalysis. We also gratefully acknowledge the contributions of many co-workers whose names are cited in the descriptions of the portions of the reviewed work that were done in our laboratory.

References

[1] H. Zuber, R.A. Brunisholz, in: H. Scheer (Ed.), Chlorophylls, CRC Press, Boca Raton, FL, 1991.
[2] D. Gosztola, M.P. Niemczyk, M.R. Wasielewski, J. Am. Chem. Soc. 120 (1998) 5118.
[3] (a) P.G. Van Patten, A.P. Shreve, J.S. Lindsey, R.J. Donohoe, J. Phys. Chem. B 102 (1998) 4209;
(b) D. Gust, T.A. Moore, A.L. Moore, Acc. Chem. Res. 26 (1993) 198;
(c) A. Harriman, J.-P. Sauvage, Chem. Soc. Rev. 25 (1996) 41.
[4] A.P. De Silva, H.Q.N. Gunaratne, T. Gunnlaugsson, A.J.M. Huxley, C.P. McCoy, J.T. Rademacher, T.E. Rice, Chem. Rev. 97 (1997) 1515.
[5] R.W. Wagner, J.S. Lindsey, J. Am. Chem. Soc. 116 (1994) 9759.
[6] (a) S. Anderson, H.L. Anderson, J.K.M. Sanders, Acc. Chem. Res. 26 (1993) 469;
(b) J. Li, A. Ambroise, S.I. Yang, J.R. Diers, J. Seth, C.R. Wack, D.F. Bocian, D. Holten, J.S. Lindsey, J. Am. Chem. Soc. 121 (1999) 8927.
[7] M.L. Merlau, M.P. Mejia, S.T. Nguyen, J.T. Hupp, Angew. Chem. Int. Ed. 40 (2001) 4239.
[8] (a) C. Sousa, C. Maziere, T.S.E. Melo, O. Vincent-Fiquet, J.C. Rogez, R. Santus, J.C. Maziere, Cancer Lett. 128 (1998) 177;
(b) W.J.A. deVree, M.C. Essers, W. Sluiter, Cancer Res. 57 (1997) 2555;
(c) A. Jasat, D. Dolphin, Chem. Rev. 97 (1997) 2267.
[9] (a) P.N. Taylor, A.P. Wylie, J. Huuskonen, H.L. Anderson, Angew. Chem. Int. Ed. Engl. 37 (1998) 986;
(b) N. Nishino, R.W. Wagner, J.S. Lindsey, J. Org. Chem. 61 (1996) 7534;
(c) R.W. Wagner, T.E. Johnson, J.S. Lindsey, J. Am. Chem. Soc. 118 (1996) 11166;
(d) A. Osuka, N. Tanabe, R.P. Zhang, K. Maruyama, Chem. Lett. (1993) 1505;
(e) D. Hammel, P. Erk, B. Schuler, J. Heinze, K. Müllen, Adv. Mater. 4 (1992) 737.
[10] (a) A. Vidal-Ferran, Z. Clyde-Watson, N. Bampos, J.K.M. Sanders, J. Org. Chem. 62 (1997) 240;
(b) S. Anderson, H.L. Anderson, J.K.M. Sanders, J. Chem. Soc. Perkin Trans. 1 (1995) 2255.
[11] Z. Xu, J.S. Moore, Acta Polym. 45 (1994) 83.
[12] C.M. Drain, F. Nifiatis, A. Vasenko, J.D. Batteas, Angew. Chem. Int. Ed. Engl. 37 (1998) 2344.
[13] H. Yuan, L. Thomas, L.K. Woo, Inorg. Chem. 35 (1996) 2808.
[14] C.M.D. Rain, K.C. Russell, J.M. Lehn, J. Chem. Soc. Chem. Commun. (1996) 337.
[15] (a) E. Iengo, R. Minatel, B. Milani, L.G. Marzilli, E. Alessio, Eur. J. Inorg. Chem. 3 (2001) 609;
(b) E. Iengo, E. Zangrando, E. Alessio, Eur. J. Inorg. Chem. (2003) 2371;
(c) S. Lo Schiavo, G. Pocsfalvi, S. Serroni, P. Cardiano, P. Piraino, Eur. J. Inorg. Chem. 6 (2000) 1371.
[16] P.C.M. van Gerven, A.A.W. Elemans, J.W. Gerritsen, S. Speller, R.J.M. Nolte, A.E. Rowan, Chem. Commun. (2005) 3535.
[17] (a) R.W. Wagner, J. Seth, S.I. Yang, D. Kim, D.F. Bocian, D. Holten, J.S. Lindsey, J. Org. Chem. 63 (1998) 5042;
(b) K.I. Sugiura, Y. Fujimoto, Y. Sakata, Chem. Commun. (2000) 1105.
[18] (a) P.J. Stang, B. Olenyuk, Acc. Chem. Res. 30 (1997) 502;
(b) M. Fujita, Chem. Soc. Rev. 27 (1998) 417.
[19] K.-I. Sugiera, Top. Curr. Chem. 228 (2003) 65.
[20] (a) M. Fujita, J. Synth. Org. Chem. Jpn. 54 (1996) 953;
(b) M. Fujita, O. Sasaki, T. Mitsuhashi, T. Fujita, J. Yazaki, K. Yamaguchi, K. Ogura, J. Chem. Soc. Chem. Commun. (1996) 1535;
(c) S.B. Lee, S.G. Hwang, D.S. Chung, H. Yun, J.-I. Hong, Tetrahedron Lett. 39 (1998) 873.
[21] C.M. Drain, J.M. Lehn, J. Chem. Soc. Chem. Commun. (1994) 2313.
[22] T. Milic, J.C. Garno, J.D. Batteas, G. Smeureanu, C.M. Drain, Langmuir 20 (2004) 3974.
[23] J. Fan, J.A. Whiteford, B. Olenyuk, M.D. Levin, P.J. Stang, E.B. Fleischer, J. Am. Chem. Soc. 121 (1999) 2741.
[24] P.J. Stang, J. Fan, B. Olenyuk, J. Chem. Soc. Chem. Commun. (1997) 1453.
[25] S. Leininger, B. Olenyuk, P.J. Stang, Chem. Rev. 100 (2000) 853.
[26] C.M. Drain, F. Nifiatis, A. Vasenko, J.D. Batteas, Angew. Chem. Int. Ed. 37 (1998) 2344.
[27] T.N. Milac, N. Chi, D.G. Yablon, G.W. Flynn, J.D. Batteas, C.M. Drain, Angew. Chem. Int. Ed. 41 (2002) 2117.
[28] C.M. Drain, J.D. Batteas, G.W. Flynn, T. Milac, N. Chi, D.G. Yablon, H. Sommers, Proc. Natl. Acad. Sci. 99 (2002) 6498.
[29] R.V. Slone, J.T. Hupp, Inorg. Chem. 36 (1997) 5422.
[30] M.H. Keefe, J.L. O'Donnell, R.C. Bailey, S.T. Nguyen, J.T. Hupp, Adv. Mater. 15 (2003) 1936.
[31] C.R. Graves, M.L. Merlau, G.A. Morris, S.T. Nguyen, J.T. Hupp, Inorg. Chem. 43 (2004) 2013.
[32] W.H. Otto, M.H. Keefe, K.E. Splan, J.T. Hupp, C.K. Larive, Inorg. Chem. 41 (2002) 6172.
[33] (a) J.K. Young, G.R. Baker, G.R. Newkome, K.F. Morris, C.S. Johnson Jr., Macromolecules 27 (1994) 3464;
(b) A. Burini, J.P. Fackler, R. Gallassi, A. Macchioni, M.A. Omary, M.A. Rawashdeh-Omary, B.R. Pietroni, S. Sabatani, C. Zuccaccia, J. Am. Chem. Soc. 124 (2002) 4570;
(c) B. Olenyuk, M.D. Levin, J.A. Whiteford, J.E. Shield, P.J. Stang, J. Am. Chem. Soc. 121 (1999) 10434.
[34] J.L. O'Donnell, Ph.D. Thesis, Chemistry Department, Northwestern University, 2005.
[35] S. Bélanger, M.H. Keefe, J. Welch, J.T. Hupp, Coord. Chem. Rev. 192 (1999) 29.
[36] L. Miljacic, L. Sarkisov, D.E. Ellis, R.Q. Snurr, J. Chem. Phys. 121 (2005) 7228.
[37] K.E. Splan, C.L. Stern, J.T. Hupp, Inorg. Chim. Acta 357 (2004) 4005.
[38] X. Chi, A.J. Guerin, R.A. Haycock, C.A. Hunter, L.D. Sarson, Chem. Commun. (1995) 2567.
[39] I.-W. Hwang, T. Kamada, T.K. Ahn, D.M. Ko, T. Nakamura, A. Tsuda, D. Kim, J. Am. Chem. Soc. 126 (2004) 16187.
[40] A. Tsuda, T. Nakamura, S. Sakamoto, K. Yamaguchi, A. Osuka, Angew. Chem. Int. Ed. 41 (2002) 2817.
[41] K. Funatsu, T. Imamura, A. Ichimura, Y. Sasaki, Inorg. Chem. 37 (1998) 1798.
[42] K. Fukushima, K. Funatsu, A. Ichimura, Y. Sasaki, M. Suzuki, T. Fujihara, K. Tsuge, T. Imamura, Inorg. Chem. 42 (2003) 3187.
[43] I.-W. Hwang, T. Kamada, T.K. Ahn, D.M. Ko, T. Nakamura, A. Tsuda, A. Osuka, D. Kim, J. Am. Chem. Soc. 126 (2004) 16187.
[44] S.H. Chang, K.B. Chung, R.V. Slone, J.T. Hupp, Synth. Met. 117 (2001) 215.
[45] D.G. Whitten, I.G. Popp, P.D. Wildes, J. Am. Chem. Soc. 90 (1968) 7196.
[46] G.A. Mines, B.C. Tzeng, K.J. Stevenson, J. Li, J.T. Hupp, Angew. Chem. Int. Ed. 41 (2002) 154.
[47] A.M.D.R. Gonsalves, M.M. Pereira, J. Mol. Catal. A 113 (1996) 209.
[48] L.A. Campbell, T. Kodadek, J. Mol. Catal. A 113 (1996) 293.
[49] M.J. Guther, P. Turner, Coord. Chem. Rev. 108 (1991) 115.
[50] K.F. Czaplewski, J.T. Hupp, R.Q. Snurr, Adv. Mater. 13 (2001) 1895.
[51] M.E. Williams, J.T. Hupp, J. Phys. Chem. B 105 (2001) 8944.
[52] S. Belanger, J.T. Hupp, Angew. Chem. Int. Ed. 38 (1999) 2222.
[53] H.E. Katz, M.L. Shilling, C.E.D. Chidsey, T.M. Putvinski, R.S. Hutton, Chem. Mater. 8 (1996) 1490.
[54] G. Cao, H.G. Hong, T.E. Mallouk, Acc. Chem. Res. 25 (1992) 420.
[55] A. Clearfield, Prog. Inorg. Chem. 47 (1998) 371.

[56] J.L. Snover, H. Byrd, E.P. Suponeva, E. Vicenzi, M.E. Thompson, Chem. Mater. 8 (1996) 1490.
[57] J. Libera, R. Gurney, C. Schwartz, H. Jin, T.L. Lee, S.T. Nguyen, J.T. Hupp, M. Bedzyk, J. Phys. Chem. B 109 (2005) 1441.
[58] L. Doron-Mor, H. Cohen, S.R. Cohen, R. Popovitz-Biro, A. Shanzer, A. Vaskevich, I. Rubinstein, Langmuir 20 (2004) 10727.
[59] K.E. Splan, A.M. Massari, J.T. Hupp, J. Phys. Chem. B 108 (2004) 4111.
[60] T. Taniguchi, Y. Fukasawa, T. Miyashita, J. Phys. Chem. B 103 (1999) 1920.
[61] K.E. Splan, A.M. Massari, J.T. Hupp, J. Phys. Chem. B 108 (2004) 4111.